

Experimental observation of bound states of 2D Dirac electrons on the surface of topological insulator Bi_2Se_3

N.I. Fedotov and S.V. Zaitsev-Zotov

Kotel'nikov IRE RAS, Mokhovaya 11, bld.7, 125009 Moscow, Russia

(Dated: May 3, 2022)

Topologically protected surface states of three-dimensional topological insulators provide a model framework for studying massless Dirac electrons in two dimensions. Massless Dirac electrons can travel without reflection through a potential step (Klein tunneling). Due to the Klein tunneling the confinement of massless fermions by means of purely electrostatic potential is not possible in a one-dimensional case. However for a 2D Dirac system with a one-dimensional potential, bound states exist for both a potential well and a potential barrier. Such potential wells are formed in the vicinity of extended defects on the surface of the topological insulator Bi_2Se_3 due to band bending. We report the observation of bound states in such potential wells in our scanning tunneling microscopy and spectroscopy investigation of the surface of the topological insulator Bi_2Se_3 .

Recently, a number of solid state systems have been used as model systems for investigating exotic particle physics for quantum field theory and high-energy physics. Of great interest in this respect are Dirac materials [1]. Their electronic excitations obey the Dirac equation, in place of the Schrödinger one. This opens up a possibility to study quasirelativistic physics in a convenient tunable solid-state setting. In particular, graphene and, more recently, topological insulators provide a model framework for studying massless Dirac electrons in two dimensions.

Three-dimensional topological insulators are characterized by the presence of gapless surface states on the background of an insulating bulk [2]. The existence of these states is governed by the nontrivial value of the \mathbb{Z}_2 invariant. Bi_2Se_3 belongs to this class of materials [3]. In Bi_2Se_3 the topologically protected surface states form a cone in k -space. The apex of the cone (the Dirac point) is located at the Γ -point of the surface Brillouin zone, its energy being within the bulk band gap. In the vicinity of the Dirac point the Bi_2Se_3 surface states can be described by a model Dirac Hamiltonian $H = A\boldsymbol{\sigma}\mathbf{k}$ [3]. Here $\boldsymbol{\sigma} = (\sigma_x, \sigma_y)$ is the Pauli matrices vector, \mathbf{k} is the wave vector, $A \approx 0.33$ eV nm defines the Fermi velocity.

Massless Dirac electrons possess a number of peculiar properties. For instance, they can travel without reflection through a potential step (Klein tunneling [4, 5]). It is generally accepted that due to the Klein tunneling the confinement of massless fermions by means of purely electrostatic potential is not possible. It is true in a one-dimensional (1D) case, however for a 2D Dirac system with a 1D potential, states localized in one direction (perpendicular to the potential well or barrier) exist [6, 7]. The issue of Dirac electrons confinement continues to attract considerable attention from theorists [8–11]. Experiments in this area have been mostly concentrated on graphene: from Klein tunneling [12] to lithographically defined quantum dots [13] and chemically synthesized flakes [14]. More recently, quasi-bound states were observed by means of scanning tunneling microscopy in electrostatically defined quantum dots [15, 16]. Current

distribution in one-dimensional graphene edge channels was investigated in transport measurements [17].

Here we report direct observation of bound states in potential wells formed in the vicinity of steps and other extended defects of the surface of the topological insulator Bi_2Se_3 . We employ scanning tunneling microscopy and spectroscopy (STM/STS) to image the spatial distribution of LDOS.

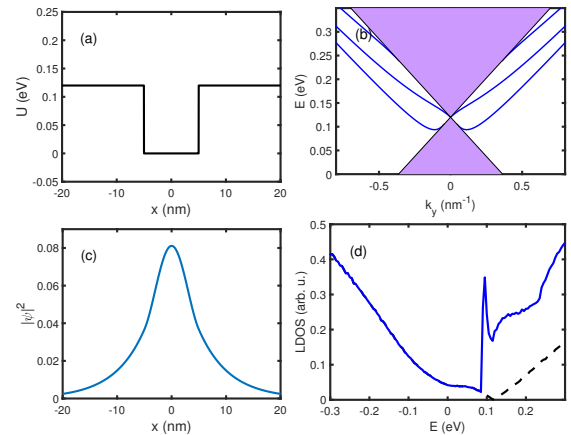


FIG. 1: Model square potential well (a). Dispersion of the bound states in the square potential well (b). A wave function of a bound state from the lowest branch in the well (c). LDOS in the middle of the rectangular potential well. Dashed line shows the contribution of the delocalized states only (d). A dI/dV curve on the surface of the topological insulator Bi_2Se_3 near a surface step (d). $T = 5$ K.

Let us briefly remind the specifics of bound states formation in a massless Dirac system using an exactly solvable model of a rectangular potential well. Following [6, 7], we are considering a system with a Hamiltonian

$$H = A\boldsymbol{\sigma}\mathbf{k} + U(x), \quad (1)$$

where U is a 1D rectangular potential well running along

the y axis (Fig. 1(a))

$$U(x, y) = \begin{cases} U, x < -l \\ 0, -l \leq x < l \\ U, l \leq x. \end{cases}$$

Since H is invariant under translations along the y axis, k_y is a good quantum number. Inside the well the wavefunction ψ is a combination of $\exp(\pm ik_x x + ik_y y)$ and outside the well $\psi \propto \exp(-Qx|x| + ik_y y)$. For k_x and $Q_x > 0$ we have $E^2 = A^2 k_x^2 + A^2 k_y^2$ and $(E - U)^2 = -A^2 Q_x^2 + A^2 k_y^2$ correspondingly. The continuity condition for the wave function at $x = \pm l$ leads to an equation for k_x of the states localized in the x direction in the quantum well

$$(EU - A^2 k_x^2) \sin 2k_x l + A^2 Q_x k_x \cos 2k_x l = 0. \quad (2)$$

For each value of k_y equation (2) has solutions $k_{xn}, n = 1, 2, \dots$, that give us branches of the bound 1D states in the potential well. Corresponding energy dispersions are given by $E_n(k_y) = A\sqrt{(k_{xn})^2 + k_y^2}$.

The dispersions of three lowest branches of these states calculated using Eq. (2) for $U = 0.12$ eV, $l = 5$ nm are shown in Fig. 1(b). The shaded area represents the continuum of the 2D states forming the Dirac cone. Attached to it are the branches of the bound 1D states. The lowest branch has a minimum, that gives rise to a pronounced peak in the density of states. The second branch is attached to the Dirac point. For a square potential such a branch exists independently of the potential strength, for a sufficiently weak potential it is the lowest branch. This may be also the case for other potential shapes as is claimed in [18].

The calculated local density of states (LDOS) in the center of the potential well is shown in Fig. 1(c) (solid line). It deviates considerably from the V-shape of the unperturbed LDOS. The minimum flattens out and a maximum appears. The contribution of delocalized states to the LDOS is shown in Fig. 1(c) by a dashed line. We see that the sharp feature is due to the local density of the bound states. The probability density $|\psi|^2$ of a bound state from the lowest branch is shown in Fig. 1(a).

Thus, the signatures of the bound states in the LDOS are disappearance and flattening of the sharp V-shaped minimum, representing the Dirac cone apex, and formation of a single or multiple peaks or step-like features (see also [10]). STM can be used to search for such features in the tunneling spectra. 1D potential wells similar to the one discussed above arise due to the band bending in the vicinity of extended surface defects of a topological insulator, *e. g.* Bi_2Se_3 . Below we report our observations of bound states in two types of such potential wells [19].

For the experimental search for the bound states we performed spatially resolved scanning tunneling microscopy and spectroscopy measurements on the surface

of Bi_2Se_3 samples cleaved *in situ*. All the measurements were done at liquid helium temperature in the UHV conditions (typical base vacuum 2×10^{-11} Torr). Pt-Rh tips were used, their quality was checked on Au foil. If needed, we performed a tip recovery procedure which included briefly dipping the tip into the Au foil followed by the tip control procedure. The dI/dV curves of the tunneling junction (tunneling spectra) were obtained by numerically differentiating measured $I(V)$ curves. To account for the band bending and extract information about the local potential we use the normalization method described in Ref. [19]. The local potential is obtained as the overall shift of the normalized dI/dV curve.

Bi_2Se_3 is a layered compound that consists of quintuple layers (QL) Se-Bi-Se-Bi-Se bound one with another by van der Waals interaction. When Bi_2Se_3 is cleaved, high steps ($\gtrsim 1$ nm) are formed if one or more quintuple layers are torn. An STM image of such a step is shown in Fig. 3(a). The step height ~ 1 nm corresponds to 1 QL. In the vicinity of these steps on Bi_2Se_3 surface on a ~ 10 nm scale a $100 - 200$ meV shift of the chemical potential occurs [19, 20], thus forming a potential well for the Dirac electrons.

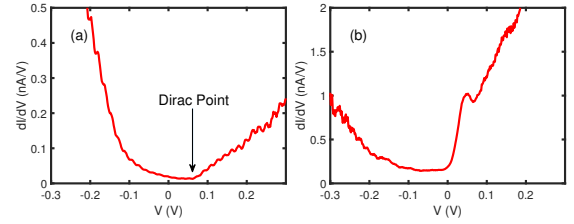


FIG. 2: A typical dI/dV curve on the surface of the topological insulator Bi_2Se_3 away from defects (a). A dI/dV curve on the surface of the topological insulator Bi_2Se_3 near a surface step (b). $T = 5$ K.

A typical differential tunneling conductance (dI/dV) curve taken far from any defects is presented in Fig. 2(a). As the Dirac point of the Bi_2Se_3 surface states lies within its bulk band gap, it corresponds to the V-shaped minimum of the dI/dV curve (shown with an arrow). A differential tunneling conductance curve taken on a step is shown in Fig. 2(b). Apart from an overall shift in voltage, corresponding to the local potential, it shows significant change in shape in comparison with the spectrum away from defects (Fig. 2(a)). Specifically, the V-shaped minimum corresponding to the Dirac point flattens out and a sharp rise with a maximum appears at the side of the flattened region of the curve. From the comparison with the model predictions it is evident, that these changes of LDOS are in agreement with the expected effect of a potential well. In particular the sharp feature corresponds to bound states formation.

A spatially resolved STS map taken along a line (black squares in Fig. 3(a)) across the step in Fig. 3(a) is shown in Fig. 3(b). Approximate positions of the Dirac point

and bulk band edges (depicted by white dashed lines in Fig. 3(b)) are determined as in Ref. [19]. A 0.15 V deep and ~ 15 nm wide potential well forms due to the band bending in the vicinity of the step (which is located at $L \approx 17$ nm). A horizontal feature of the normalized dI/dV appears in the potential well region at $V \approx 0.02$ eV. This feature in the STS map corresponds to a maximum of the differential tunneling conductance, such as the one in Fig. 2(b). We argue that this horizontal feature is evidence of formation of bound states in a system of massless 2D electrons, namely the topologically protected surface states of a topological insulator.

To justify our interpretation we compare the experimental spatially resolved STS data in the potential wells near extended surface defects with the spatial distributions of numerically calculated local density of states of 2D massless Dirac electrons in a one-dimensional potential $U(x)$ of the same shape. We perform our calculations based on the model Dirac Hamiltonian Eq (1). The potential U is assumed to be constant along the y axis in our approximation, so that the wave function $\Psi(x, y) = \psi(x)e^{ik_y y}$ and the 2D Dirac equation is reduced to a 1D equation for each value of k_y . We numerically solve the corresponding equation by a symmetric finite difference method with periodical boundary conditions. Grid discretizations of such equations produce spurious solutions, a problem known as fermion doubling. One of the ways to avoid the fermion doubling is to add a Wilson mass term $wk^2\sigma_z$ [21]. This is the method we use in this work.

The numerically calculated spatial distribution of the local density of states in the quantum well, corresponding to the potential near the step in Fig. 3(a), is shown in Fig. 3(c). The white dashed line depicts the potential profile used for the calculations. The results are in reasonable quantitative as well as quantitative agreement with the experimental dI/dV distribution both in energy and in space. Namely, a sharp feature appears in the potential well region in the calculations as well as in the experimental results. The energy dispersion $E(k_y)$ resulting from the numerical simulation exhibits similar features as the one in Fig. 1(b). Namely, branches of bound states arise, attached to the Dirac cone of the 2D delocalized states. The local density of these states produces the horizontal feature in the spatial distribution of LDOS.

Apart from the steps, the STM measurements reveal other extended defects on the Bi_2Se_3 surface. An STM image of a line defect of such kind is shown in Fig. 4(a). The defect appears as a linear protrusion of height ~ 0.1 nm and width ~ 10 nm. We interpret it as a manifestation of some kind of buried defect, such as a grain (or domain) boundary [22]. A spatially resolved STS map taken along a line (black squares in Fig. 4(a)) across this defect is shown in Fig. 4(b). Approximate positions of the Dirac point and bulk band edges (depicted by white

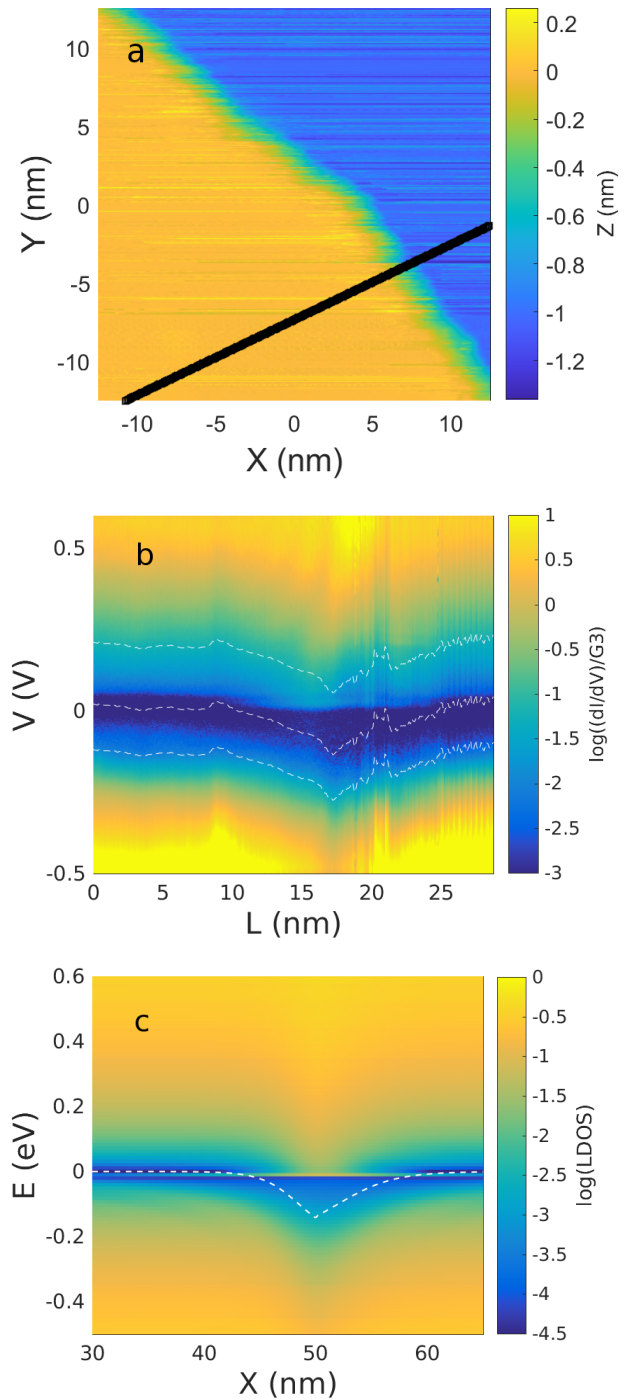


FIG. 3: STM image of a step on the Bi_2Se_3 surface. black squares represent the points where $I(V)$ curves were taken (a). Normalized differential tunneling conductance along the line across the step on the Bi_2Se_3 surface. White dashed lines represent approximate positions of the Dirac point and bulk band edges (b). LDOS obtained from numerical calculations for the potential (white dashed line) approximating the potential landscape near the step on the Bi_2Se_3 surface (c)

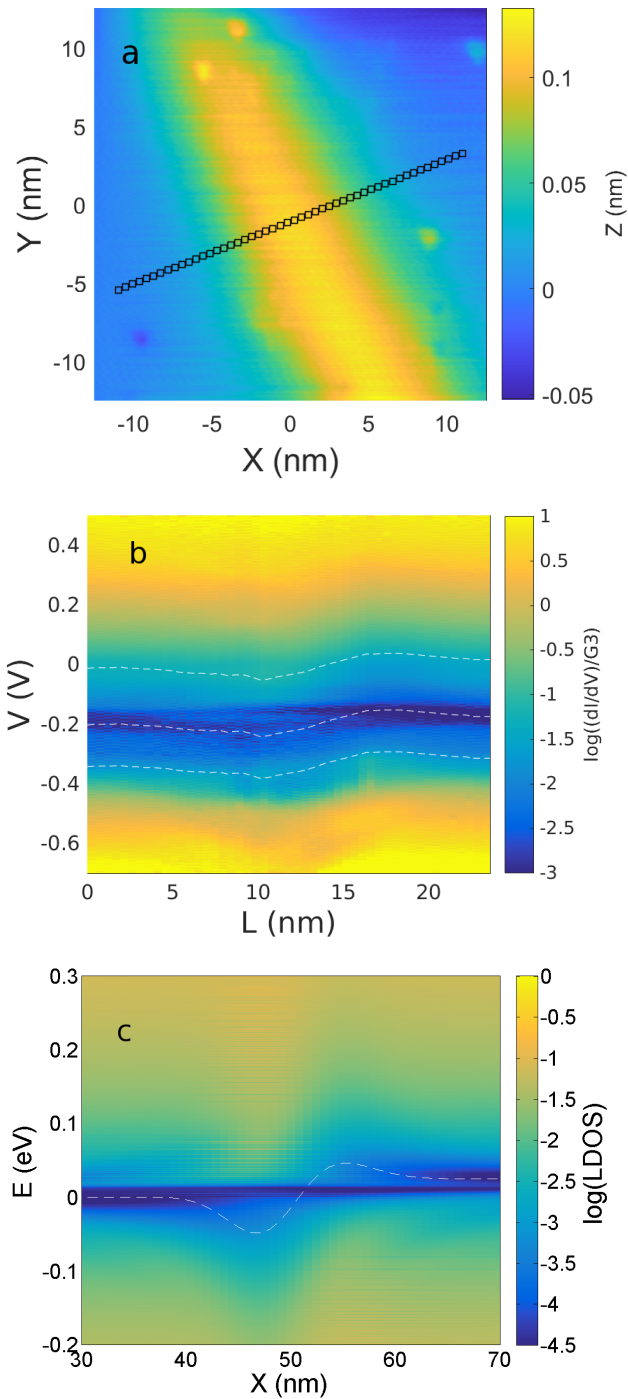


FIG. 4: STM image of a linear defect on the Bi_2Se_3 surface. black squares represent the points where $I(V)$ curves were taken (a). Normalized differential tunneling conductance along the line across the linear defect on the Bi_2Se_3 surface. White dashed lines represent approximate positions of the Dirac point and bulk band edges (b). LDOS obtained from numerical calculations for the potential (white dashed line) approximating the potential landscape near the linear defect on the Bi_2Se_3 surface (c).

dashed lines in Fig. 4(b)) are determined as in Ref. [19]. The potential landscape in the area of the defect comprises a potential well of depth $U \approx 0.07$ eV and width $l \approx 10$ nm. At $V \approx -0.18$ V a horizontal maximum in the differential tunneling conductance appears in the potential well region, as in the case of the surface step.

The corresponding numerically calculated LDOS distribution is shown in Fig. 4(c) along with the potential profile used for the calculation (white dashed line). Again, we see the formation of a sharp LDOS feature in the potential well in accordance with Fig. 4(b) due to the bound states.

The formation of such bound states (or waveguide states) was discussed theoretically in [8, 9] in the case of topological insulators. These two papers focus on the branches of the bound states that connect to the Dirac point. We find that for the typical parameters of the potential wells in our case (100 mV, 10 nm) lower lying branches exist, that provide a larger peak-like contribution to the LDOS. Notably, energy dispersion and properties of such states depend on the parameters of the potential and may vary *e. g.* with step height or defect type.

In contrast with other papers [23, 24], where the surface step is modeled as a scattering δ -function barrier, we are considering only the experimentally observed potential wells formed on both sides of the step. The rationale behind this approach is that the topologically protected surface states flow around the step. To take the effect of the step into account more accurately one needs to consider a three-dimensional model.

The formation of bound states at the extended defects of the surface (especially surface steps) of topological insulators may result in additional conductivity and scattering channels and has to be taken into account when considering prospects of topological insulator-based quantum devices. Finally, spin texture associated with such a defects is an interesting question.

In conclusion, we experimentally observe formation of one-dimensional bound states of two-dimensional massless Dirac electrons in potential wells due to band bending in the vicinity of extended surface defects in the Bi_2Se_3 topological insulator. Numerical simulations support this conclusion and provide a recipe for their identification. The states form branches attached to the Dirac cone and can be identified on spatially resolved STS maps as sharp horizontal features.

Acknowledgements. We are grateful to V.A. Sablikov for valuable discussion. The work was carried out with financial support of RSF (grant 16-12-10335).

- [2] As a review see: Topological Insulators: Fundamentals and Perspectives, Eds.: Frank Ortmann, Stephan Roche, Sergio O. Valenzuela, Laurens W. Molenkamp, Wiley (2015); Contemporary Concepts of Condensed Matter Science, Eds.: E.Burstein, A.H. Macdonald and P. J. Stiles, Vol. 6, Topological Insulators, Eds.: M. Franz, L. Molenkamp, Elsevier, Oxford, 2013.
- [3] Haijun Zhang, Chao-Xing Liu, Xiao-Liang Qi, Xi Dai, Zhong Fang and Shou-Cheng Zhang, *Nat. Phys.* **5**, 438–442 (2009).
- [4] Klein, O. *Z. Phys.* **53**, 157 (1929).
- [5] M. I. Katsnelson, K. S. Novoselov, and A. K. Geim *Nat. Phys.* **2**, 620–625 (2006).
- [6] J. Milton Pereira, Jr., V. Mlinar, F. M. Peeters, and P. Vasilopoulos *Phys. Rev. B* **74**, 045424 (2006).
- [7] T. Ya. Tudorovskiy, A. V. Chaplik, *JETP Lett.* **84**, 619 (2007).
- [8] Takehito Yokoyama, Alexander V. Balatsky, and Naoto Nagaosa *Phys. Rev. Lett.* **104**, 246806 (2010).
- [9] Ranjani Seshadri and Diptiman Sen *Phys. Rev. B* **89**, 235415 (2014).
- [10] V A Yampol'skii, S Savel'ev and Franco Nori, *New J. Phys.* **10**, 053024 (2008).
- [11] R. R. Hartmann and M. E. Portnoi *Scientific Reports* **7**, 11599 (2017).
- [12] Young, A. F. and Kim, P. *Nat. Phys.* **5**, 222–226 (2009).
- [13] L. A. Ponomarenko, *et al.* *Science* **320**, 356–358 (2008).
- [14] D. Subramaniam, F. Libisch, Y. Li, C. Pauly, V. Geringer, R. Reiter, T. Mashoff, M. Liebmann, J. Burgdörfer, C. Busse, T. Michely, R. Mazzarello, M. Pratzer, and M. Morgenstern *Phys. Rev. Lett.* **108**, 046801 (2012).
- [15] Christopher Gutiérrez, Lola Brown, Cheol-Joo Kim, Ji-woong Park, and Abhay N. Pasupathy *Nat. Phys.* **12**, 1069 (2016).
- [16] Juwon Lee, Dillon Wong, Jairo Velasco Jr, Joaquin F. Rodriguez-Nieva, Salman Kahn, Hsin-Zon Tsai, Takashi Taniguchi, Kenji Watanabe, Alex Zettl, Feng Wang, Leonid S. Levitov, and Michael F. Crommie *Nat. Phys.* **12**, 1032 (2016).
- [17] M. T. Allen, O. Shtanko, I. C. Fulga, A. R. Akhmerov, K. Watanabe, T. Taniguchi, P. Jarillo-Herrero, L. S. Levitov, and A. Yacoby *Nat. Phys.* **12**, 128 (2016).
- [18] Yishuai Xu, Guodong Jiang, Janet Chiu, Lin Miao, Erica Kotta, Yutan Zhang, Rudro R. Biswas, and L. Andrew Wray, arXiv:1804.07841.
- [19] N. I. Fedotov and S. V. Zaitsev-Zotov *Phys. Rev. B* **95**, 155403 (2017).
- [20] A.Yu. Dmitriev, N.I. Fedotov, V.F. Nasretdinova, S.V. Zaitsev-Zotov, Pis'ma Zh. Eksp. Teor. Fiz., **100**, 442 (2014); JETP Letters, **100**, 398 (2014). DOI: 10.1134/S0021364014180039.
- [21] Leonard Susskind *Phys. Rev. D* **16**, 3031 (1977).
- [22] Y. Liu, Y. Y. Li, D. Gilks, V. K. Lazarov, M. Weinert, and L. Li *Phys. Rev. Lett.* **110**, 186804 (2013).
- [23] R. Biswas and Alexander V. Balatsky *Phys. Rev. B* **83**, 075439 (2011).
- [24] Jin An and C. S. Ting *Phys. Rev. B* **86**, 165313 (2012).